Sample-Spaced and Fractionally-Spaced CIR Estimation Aided Decision Directed Channel Estimation for OFDM and MC-CDMA

J. Akhtman and L. Hanzo
School of ECS., Univ. of Southampton, SO17 1BJ, UK.
Tel: +44-23-80-593 125, Fax: +44-23-80-593 045
Email: lh@ecs.soton.ac.uk, http://www-mobile.ecs.soton.ac.uk

***Abstract*— The achievable performance of decision-directed channel estimation (DDCE) is analysed in the context of both OFDM and MC-CDMA systems. Two different estimation methods suitable for both OFDM and MC-CDMA systems are considered, which employ sample-spaced (SS) as well as fractionally-spaced (FS) *a posteriori* channel impulse response (CIR) estimators. The performance of both estimation methods is compared and it is shown that the DDCE scheme employing the FS-CIR estimator outperforms its SS-CIR estimator-based counterpart. Furthermore, the FS-CIR estimator-based method exhibits higher robustness to various channel parameters such as the channel's root mean square delay spread. Finally, it is shown that the MC-CDMA system employing the channel estimation scheme advocated outperforms its OFDM counterpart.**

I. Introduction

The ever-increasing demand for high data rates in wireless networks requires the efficient utilisation of the limited bandwidth available, while supporting a high grade of mobility in diverse propagation environments. Orthogonal Frequency Devision Multiplexing (OFDM) and Multi-Carrier Code Devision Multiple Access (MC-CDMA) techniques [1] are capable of satisfying these requirements, since they are capable of coping with highly time-variant wireless channel characteristics. However, the capacity and the achievable integrity of communication systems is highly dependent on the system's knowledge concerning the channel conditions encountered. Thus, the provision of an accurate and robust channel estimation strategy is a crucial factor in achieving a high performance.

A *decision directed* channel estimation (DDCE) method suitable for both OFDM and MC-CDMA systems was proposed in [2]. The estimator derived in [2] assumes a channel characterized by a Sample-Spaced Channel Impulse Response (SS-CIR). However, it is evident that this assumption cannot be sustained in realistic channel conditions. Hence, in this contribution we analyse the achievable performance of the estimation method proposed in [2] in conjunction with a more realistic Fractionally-Spaced (FS) CIR-based channel model. Furthermore, we propose an enhanced DDCE scheme evolving from that in [2], resulting in an *a posteriori* FS-CIR estimator in contrast to the SS-CIR estimator derived in [2]. We then perform a comparison between the two methods considered and demonstrate the advantages of the newly proposed scheme.

The rest of this paper is structured as follows. The channel model and the corresponding system model are described in Section II. The Reduced Complexity (RC) MMSE SS-CIR estimator introduced in [2] is derived in Section III-B. The FS version of the *a posteriori* CIR estimator proposed is derived in Section III-C. Finally, The performance of both methods considered is compared using extensive computer simulations and the corresponding results are demonstrated in Section IV, before concluding in Section V.

Acknowledgements: The work reported in this paper has formed part of the Wireless Enabling Techniques work area of the Core 3 Research Programme of the Virtual Centre of Excellence in Mobile and Personal Communications, Mobile VCE, www.mobilevce.com, whose funding support, including that of EPSRC, is gratefully acknowledged. Fully detailed technical reports on this research are available to Industrial Members of Mobile VCE.

II. System Model

A. Channel Statistics

A Single Input Single Output (SISO) wireless communication link is constituted by a multiplicity of statistically independent components, termed as *paths*. Thus, such a channel is referred to as a *multipath* channel. The physical interpretation of each individual path is a single distortionless ray between the transmitter and the receiver antennas.

The individual scattered and delayed signal components usually arise as a result of refraction or diffraction from scattering surfaces. In most recently proposed wireless mobile channel models each such CIR component α_l associated with an individual channel path is modelled by a wide sense stationary (WSS) narrow-band complex Gaussian process [3] having correlation properties characterised by the cross-correlation function

$$r_\alpha[m,j] = E\{\alpha_i[n]\alpha_j^*[n-m]\} = r_{t;i}[m]\delta[i-j] \ , \qquad (1)$$

where n is a discrete OFDM-block-related time-domain index and $\delta[\cdot]$ is the Kronecker delta function. The above equation suggests that the different CIR components are assumed to be mutually uncorrelated and each exhibits time-domain autocorrelation properties defined by the time-domain correlation function $r_{t;i}[m]$. The Fourier transform pair of the correlation function $r_t[n]$ associated with each CIR tap corresponds to a band-limited power spectral density (PSD) $p_t(f)$, such that we have $p_t(f) = 0$, if $|f| > f_d$, where f_d is termed as the *maximum Doppler frequency*. The time period $1/f_d$ is the so-called *coherence time* of the channel [3] and usually we have: $1/f_d \gg T$, where T is the duration of the OFDM block.

We adopt the complex baseband representation of the continuous-time Channel Impulse Response (CIR) given by [3]

$$h(t,\tau) = \sum_l \alpha_l(t)c(\tau-\tau_l), \qquad (2)$$

where $\alpha_l(t)$ is the time-variant complex amplitude of the lth path and τ_l is the corresponding path delay, while $c(\tau)$ is the aggregate impulse response of the transmitter-receiver pair, which usually corresponds to the raised-cosine Nyquist filter. From (2) the continuous channel transfer function can be described as

$$\begin{aligned} H(t,f) &= \int_{-\infty}^{\infty} h(t,\tau)\ e^{-\jmath 2\pi f\tau} d\tau \\ &= C(f)\sum_l \alpha_l(t)e^{-\jmath 2\pi f\tau_l}, \end{aligned} \qquad (3)$$

where $C(f)$ is the Fourier transform pair of the transceiver's impulse response $c(\tau)$.

As it was pointed out in [4], in OFDM/MC-CDMA systems using a sufficiently long cyclic prefix and adequate synchronisation, the discrete subcarrier-related CTF can be expressed as

$$H[n,k] \triangleq H(nT, k\Delta f) = C(k\Delta f) \sum_{l=1}^{L} \alpha_l[n] W_K^{k\tau_l/T_s} \quad (4)$$

$$= \sum_{m=0}^{K_0-1} h[n,m] W_K^{km}, \quad (5)$$

where

$$h[n,m] \triangleq h(nT, mT_s) = \sum_{l=1}^{L} \alpha_l[n] c(mT_s - \tau_l) \quad (6)$$

is the Sample-Spaced CIR (SS-CIR) and we have $W_K = \exp(-\jmath 2\pi/K)$. Note that in realistic channel conditions associated with non-sample-spaced time-variant path-delays $\tau_l(n)$ the receiver will encounter dispersed received signal components in several neighbouring samples owing to the convolution of the transmitted signal with the system's impulse response, which we refer to as leakage. This phenomenon is usually unavoidable and therefore the resultant SS-CIR $h[n,m]$ will be constituted of numerous correlated non-zero taps described by Equation (2) and illustrated in Figure 1. By contrast, the fractionally-spaced CIR (FS-CIR) $\alpha_l[n] \triangleq \alpha_l(nT)$ will be constituted by a lower number of $L \ll K_0 \ll K$ statistically independent non-zero taps associated with distinctive propagation paths, as depicted in Figure 1.

As it was shown in [4], the crosscorrelation function $r_H[m,l]$, which characterized both the time- and frequency-domain correlation properties of the discrete CTF coefficients $H[n,k]$ associated with different OFDM blocks and subcarriers can be described as

$$r_H[m,l] \triangleq E\{H[n+m,k+l]H^*[n,k]\} = \sigma_H^2 r_t[m] r_f[l], \quad (7)$$

where $r_t[m]$ is the time-domain correlation function of Equation (1), while $r_f[i]$ is the frequency-domain correlation functions, which can be expressed as in [5]

$$r_f[l] = |C(l\Delta f)|^2 \sum_{i=1}^{L} \frac{\sigma_i^2}{\sigma_H^2} e^{-\jmath 2\pi l \Delta f \tau_i}, \quad (8)$$

where $\sigma_H^2 = \sum_{i=1}^{L} \sigma_i^2$.

B. MC Transceiver

The discrete frequency-domain model of the OFDM/MC-CDMA system can be described as

$$y[n,k] = H[n,k]x[n,k] + w[n,k], \quad (9)$$

for $k = 0, \ldots, K-1$ and all n, where $y[n,k], x[n,k]$ and $w[n,k]$ are the received symbol, the transmitted symbol and the Gaussian noise sample respectively, corresponding to the kth subcarrier of the nth OFDM block. Furthermore, $H[n,k]$ is the complex channel transfer function (CTF) coefficient associated with the kth subcarrier and time instance n. Note that in the case of an M-QAM modulated OFDM system, $x[n,k]$ corresponds to the M-QAM symbol accommodated by the kth subcarrier, while in a MC-CDMA system, such as a Walsh-Hadamard Transform (WHT) assisted OFDM scheme using G-chip WH spreading code and hence capable of supporting G users [1] we have

$$x[n,k] = \sum_{p=0}^{G-1} c[k,p] s[n,p], \quad (10)$$

where $c[k,p]$ is the kth chip of the pth spreading code, while $s[n,p]$ is the M-QAM symbol spread by the pth code. Each of the G spreading codes is constituted by G chips.

III. Channel Estimation

A. Decision Directed Channel Estimator

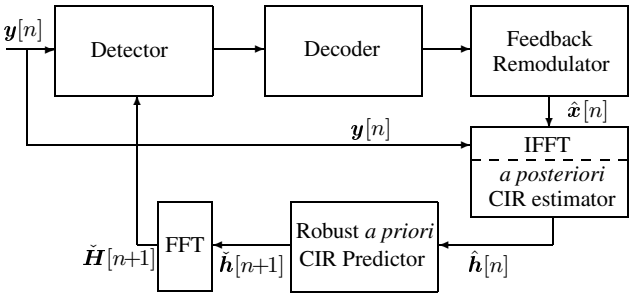

Fig. 2. Schematic of the channel estimator constituted by an *a posteriori* decision-directed CIR estimator, based on frequency-domain modulated symbol estimates, followed by an *a priori* CIR predictor.

The schematic of the channel estimation method considered is depicted in Figure 2. Our channel estimator is constituted by what we refer to as an *a posteriori* decision-directed CIR estimator followed by an *a priori* CIR predictor [1]. As seen in Figure 2, the task of the CIR estimator is to estimate the CIR taps corresponding to the current channel state based on the *a posteriori* information about the received subcarrier-related information-carrying symbols. We employ a linear Reduced Complexity (RC) MMSE estimator described in [2], which invokes an Inverse Fourier Transform based transformation from the subcarrier-related frequency domain to the CIR-related time domain in order to exploit the frequency-domain correlation of the subcarrier-related CTF coefficients.

As seen in Figure 2, the *a posteriori* CIR estimator inputs are the received subcarrier-related frequency-domain signal $\boldsymbol{y}[n]$ and the decision-based estimate $\hat{\boldsymbol{x}}[n]$. Its output is an *a posteriori* estimate $\hat{\boldsymbol{h}}[n]$ of the CIR taps, which is fed into the low-rank time-domain CIR tap predictor of Figure 2 for the sake of producing an *a priori* estimate $\check{h}[n+1, l],\ l = 0, 1, \cdots, K_0 - 1$ of the next CIR on a CIR tap-by-tap basis [1]. Finally, the predicted CIR is converted to the FD-CTF with the aid of the Fourier Transform block of Figure 2. The resultant FD-CTF is employed by the receiver for the sake of detecting and decoding of the next OFDM symbol. Note, that this principle requires the transmission of a pilot-based channel sounding sequence, such as for example in FD pilot-assisted OFDM, during the initialisation stage.

In our DDCE scheme of Figure 2 we employ the Robust *a priori* CIR predictor introduced in [4], whicch is detailed in [1].

B. RC-MMSE SS-CIR Estimator

In this section we present a brief description of the *a posteriori* Reduced Complexity (RC) MMSE Sample-Spaced (SS) CIR estimator advocated in [2]. Our estimator is comprised of a temporary scalar MMSE CTF estimator followed by a simplified MMSE SS-CIR estimator.

Following the Bayesian linear model theory of [6], the temporary MMSE estimator of the FD-CTF coefficients $H[n,k]$ of the scalar linear model described by Equation (9), where the parameters $H[n,k]$ are assumed to be complex-Gaussian distributed with a zero mean

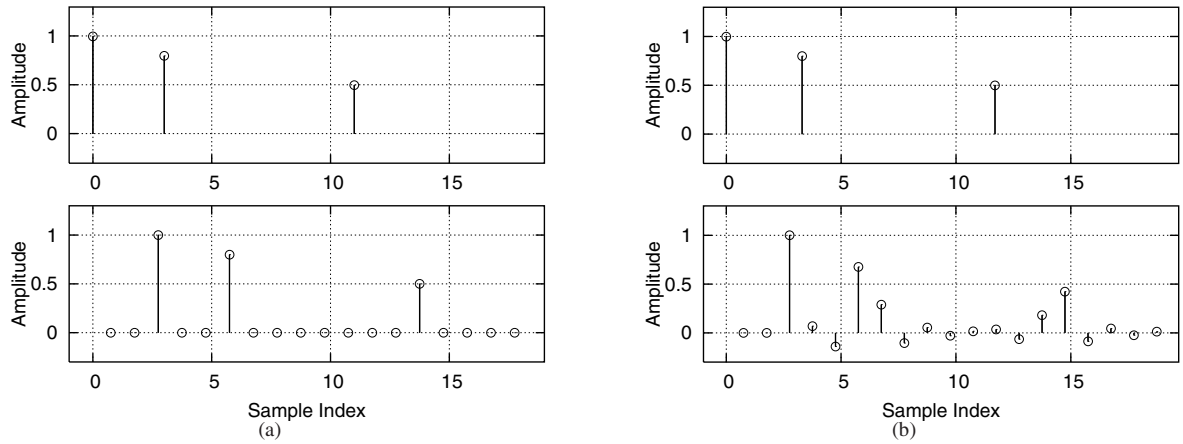

Fig. 1. The **FS-CIR** (top) and the effective **SS-CIR** (bottom) resulting from the convolution of the original FS-CIR with the raised cosine filter impulse response for the cases of (a) sample-spaced and (b) fractionally-spaced power delay profiles.

and a variance of σ_H^2, is given by [6]:

$$\tilde{H}[n,k] = \left(\frac{x^*[n,k]x[n,k]}{\sigma_w^2} + \frac{1}{\sigma_H^2}\right)^{-1} \cdot \frac{x^*[n,k]y[n,k]}{\sigma_w^2} = \frac{x^*[n,k]y[n,k]}{|x[n,k]|^2 + \frac{\sigma_w^2}{\sigma_H^2}}. \quad (11)$$

The corresponding NMSE can be expressed as [6]

$$NMSE_H = \frac{1}{\sigma_H^2}\left(\frac{1}{\sigma_H^2} + \frac{|x[n,k]|^2}{\sigma_w^2}\right)^{-1} = \frac{\sigma_w^2}{\sigma_H^2|x[n,k]|^2 + \sigma_w^2} = \frac{1}{\gamma\left|\frac{x[n,k]}{\sigma_x}\right|^2 + 1}, \quad (12)$$

where

$$\gamma = \frac{1}{\sigma_w^2} E\left\{H[n,k]x[n,k]\right\} = \frac{\sigma_H^2\sigma_x^2}{\sigma_w^2} \quad (13)$$

is the average SNR level. As it is shown in [2], the NMSE of the MMSE estimator of Equation (11) is upper-bounded, by the NMSE encountered when the transmitted subcarrier-related samples $x[n,k]$ are complex-Gaussian distributed, as in the case of a MC-CDMA system having a sufficiently high spreading factor. More explicitly

$$NMSE_{H;\max}(\gamma) \leq \frac{1}{\gamma}\, \mathrm{e}^{\frac{1}{\gamma}} \mathrm{Ei}\left(\frac{1}{\gamma}\right), \quad (14)$$

where we define the *exponential integral* function as:

$$\mathrm{Ei}(x) = \int_x^\infty \frac{\mathrm{e}^{-t}}{t}\, \mathrm{d}t. \quad (15)$$

The MMSE CTF estimates $\tilde{H}[n,k]$ of Equation (11) can be now modelled as complex Gaussian-distributed variables having a mean identical to that of $H[n,k]$, which represents the actual FD-CTF coefficients encountered and a variance of $\sigma_v^2 = \sigma_H^2 NMSE_{H;\max}$, where σ_H^2 is the average channel output power and $NMSE_{H;\max}$ is the NMSE quantified in Equation (14). Thus we can write

$$\tilde{H}[n,k] = H[n,k] + v[n,k], \quad (16)$$

where $v[n,k]$ represents the i.i.d. complex-Gaussian noise samples having a zero mean and a variance of σ_v^2.

By substituting the FD-CTF of Equation (5) into (16) we arrive at

$$\tilde{H}[n,k] = \sum_{l=0}^{K_0-1} W_K^{kl} h[n,k] + v[n,k], \quad (17)$$

where $W_K \triangleq e^{-\jmath 2\pi \frac{1}{K}}$, which can be rewritten in matrix form as

$$\tilde{\boldsymbol{H}}[n] = \boldsymbol{W}\boldsymbol{h}[n] + \boldsymbol{v}[n], \quad (18)$$

where the $(K\times K_0)$-dimensional matrix $\boldsymbol{W}$ corresponds to the Fourier transform of the zero-padded SS-CIR vector $\boldsymbol{h}[n]$ and is defined by $W_{kl} \triangleq W_K^{kl}$ for $k = 0, 1, \cdots, K-1$ and $l = 0, 1, \cdots, K_0 - 1$.

The MMSE estimator of the SS-CIR taps $h[n,m]$ of the linear vector model described by Equation (18) is given by [6]

$$\hat{\boldsymbol{h}} = (\boldsymbol{C}_h^{-1} + \boldsymbol{W}^{\mathrm{H}}\boldsymbol{C}_v^{-1}\boldsymbol{W})^{-1}\boldsymbol{W}^{\mathrm{H}}\boldsymbol{C}_v^{-1}\tilde{\boldsymbol{H}}, \quad (19)$$

where we omit the time-domain OFDM-block-spaced index n for the sake of notational simplicity and define $\boldsymbol{C}_h$ and $\boldsymbol{C}_v$ as the covariance matrices of the SS-CIR vector $\boldsymbol{h}$ and the scalar-MMSE FD-CTF estimator's noise vector $\boldsymbol{v}$, respectively. The elements of the noise vector $\boldsymbol{v}$ are assumed to be complex-Gaussian i.i.d. samples and therefore we have $\boldsymbol{C}_v = \sigma_v^2\boldsymbol{I}$. On the other hand, as follows from the assumption of having uncorrelated SS-CIR taps, the SS-CIR taps' covariance matrix is a diagonal matrix $\boldsymbol{C}_h = \mathrm{diag}\left(\sigma_l^2\right)$, where $\sigma_l^2 \triangleq E\left\{|h[n,l]|^2\right\}$. Substituting $\boldsymbol{C}_h$ and $\boldsymbol{C}_v$ into Equation (19) yields

$$\hat{\boldsymbol{h}} = \left(\mathrm{diag}\left(\frac{1}{\sigma_l^2}\right) + \frac{1}{\sigma_v^2}\boldsymbol{W}^{\mathrm{H}}\boldsymbol{W}\right)^{-1} W^{\mathrm{H}}\frac{1}{\sigma_v^2}\tilde{\boldsymbol{H}} = \mathrm{diag}\left(\frac{\sigma_l^2}{\sigma_v^2 + K\sigma_l^2}\right)\boldsymbol{W}^{\mathrm{H}}\tilde{\boldsymbol{H}}, \quad (20)$$

where we have exploited the fact that

$$[\boldsymbol{W}^{\mathrm{H}}\boldsymbol{W}]_{l,l'} = \sum_{k=0}^{K-1} e^{-\jmath 2\pi \frac{k(l-l')}{K}} = K\delta[l-l'] \quad (21)$$

and therefore $\boldsymbol{W}^{\mathrm{H}}\boldsymbol{W} = K\boldsymbol{I}$, where $\boldsymbol{I}$ is a $(K_0 \times K_0)$-dimensional identity matrix.

Finally, upon substituting Equation (11) into Equation (20) we arrive at a scalar expression for the Reduced-Complexity (RC) *a*

posteriori MMSE SS-CIR estimator in the form of:

$$\hat{h}[n,l] = \frac{\sigma_l^2}{\sigma_v^2 + K\sigma_l^2} \sum_{k=0}^{K-1} W_K^{kl} \frac{\hat{x}^*[n,k]y[n,k]}{|\hat{x}[n,k]|^2 + \frac{\sigma_w^2}{\sigma_H^2}}. \quad (22)$$

The corresponding NMSE associated with the lth RC-MMSE SS-CIR tap estimate $\hat{h}[l]$ is given by [6]

$$\begin{aligned} NMSE_l &= \frac{\sigma_v^2}{\sigma_H^2} \frac{\sigma_l^2}{\sigma_v^2 + K\sigma_l^2} \\ &= \frac{\sigma_v^2}{\sigma_H^2} \frac{1}{\frac{\sigma_v^2}{\sigma_l^2} + K}, \end{aligned} \quad (23)$$

where $\sigma_v^2 = \sigma_H^2 NMSE_{H,\max}$ is the variance of the noise samples $v[k]$ in Equation (16), while $NMSE_{H,\max}$ is the maximum NMSE of the scalar MMSE FD-CTF estimator of Equation (11). The overall NMSE corresponding to the MMSE SS-CIR estimator of Equation (22) can be found by summing all of the lth contributions quantified by Equation (23) over the K_0 taps of the SS-CIR encountered, which can be expressed using Equation (14) as

$$\begin{aligned} NMSE_h &= \frac{1}{\gamma} \exp\frac{1}{\gamma} \mathrm{Ei} \frac{1}{\gamma} \sum_{l=0}^{K_0-1} \frac{1}{\frac{\sigma_v^2}{\sigma_l^2} + K} \\ &\approx \frac{1}{\gamma} \exp\frac{1}{\gamma} \mathrm{Ei} \frac{1}{\gamma} \frac{L_{\mathrm{ss}}}{K}, \end{aligned} \quad (24)$$

where, as before, K is the number of OFDM subcarriers and γ is the average SNR value, while L_{ss} is the number of non-zero SS-CIR taps encountered.

In the next section we would like to derive an alternative Reduced Complexity (RC) MMSE estimator, which is capable of estimating the Fractionally-Spaced (FS) CIR taps of Equation (5) using an approach similar to that described above.

C. MMSE FS-CIR Estimator

The first constituent component of our estimator, namely the scalar MMSE CTF estimator is identical to that derived in Section III-B and described by Equation (11). Furthermore, our approach used for deriving the MMSE FS-CIR estimator is similar to that utilized in Section III-B, however it exhibits several substantial differences, as detailed bellow.

By substituting the FD-CTF of Equation (5) into (16) we arrive at

$$\tilde{H}[n,k] = C(k\Delta f) \sum_{l=1}^{L} \alpha_l[n] W_K^{k\tau_l/T_s} + v[n,k], \quad (25)$$

where, as previously, $C(f)$ is the frequency response of the transceiver's pulse-shaping filter, $W_K \triangleq e^{-\jmath 2\pi \frac{1}{K}}$, while $\alpha_l[n]$ and τ_l are the amplitudes and the relative delays of the FS-CIR taps, respectively. Equation (25) can be expressed in a matrix form as

$$\begin{aligned} \tilde{\boldsymbol{H}}_{\mathrm{MMSE}}[n] &= \mathrm{diag}\left(C[k]\right) \boldsymbol{W} \boldsymbol{\alpha}[n] + \boldsymbol{v}[n] \\ &= \boldsymbol{T}\boldsymbol{\alpha}[n] + \boldsymbol{v}[n], \end{aligned} \quad (26)$$

where we define the $(K \times L)$-dimensional matrix $\boldsymbol{T} \triangleq \mathrm{diag}\left(C[k]\right) \boldsymbol{W}$, in which $\mathrm{diag}\left(C[k]\right)$ is a $(K \times K)$-dimensional diagonal matrix with the corresponding elements of the vector $C[k]$ on the main diagonal, while $\boldsymbol{W}$ is the Fourier Transform matrix defined by $W_{kl} \triangleq W_K^{k\frac{\tau_l}{T_s}}$ for $k = -\frac{K}{2}, \cdots, \frac{K}{2} - 1$ and $l = 1, \cdots, L$.

The MMSE estimator of the FS-CIR taps $\alpha_l[n]$ of the linear vector model described by (26) is given by [6]

$$\hat{\boldsymbol{\alpha}} = (\boldsymbol{C}_\alpha^{-1} + \boldsymbol{T}^{\mathrm{H}} \boldsymbol{C}_v^{-1} \boldsymbol{T})^{-1} \boldsymbol{T}^{\mathrm{H}} \boldsymbol{C}_v^{-1} \tilde{\boldsymbol{H}}, \quad (27)$$

where we omit the time-domain OFDM-block-spaced index n for the sake of notational simplicity and define $\boldsymbol{C}_\alpha$ and $\boldsymbol{C}_v$ as the covariance matrices of the FS-CIR vector $\boldsymbol{\alpha}$ and CTF-estimator noise vector $\boldsymbol{v}$, respectively. The elements of the noise vector $\boldsymbol{v}$ are assumed to be independent identically distributed (i.i.d.) complex-Gaussian-distributed samples and therefore we have $\boldsymbol{C}_v = \sigma_v^2 \boldsymbol{I}$. On the other hand, as follows from Equation (1), the FS-CIR taps' covariance matrix is a diagonal matrix $\boldsymbol{C}_h = \mathrm{diag}\left(\sigma_l^2\right)$, where $\sigma_l^2 \triangleq E\left\{|\alpha_l[n]|^2\right\}$. Substituting $\boldsymbol{C}_\alpha$ and $\boldsymbol{C}_v$ into (27) yields

$$\begin{aligned} \hat{\boldsymbol{\alpha}} &= \left(\mathrm{diag}\left(\frac{1}{\sigma_l^2}\right) + \frac{1}{\sigma_v^2} \boldsymbol{T}^{\mathrm{H}} \boldsymbol{T}\right)^{-1} \boldsymbol{T}^{\mathrm{H}} \frac{1}{\sigma_v^2} \tilde{\boldsymbol{H}} \\ &= \left(\sigma_v^2 \boldsymbol{I} + \mathrm{diag}\left(\sigma_l^2\right) \boldsymbol{T}^{\mathrm{H}} \boldsymbol{T}\right)^{-1} \mathrm{diag}\left(\sigma_l^2\right) \boldsymbol{T}^{\mathrm{H}} \tilde{\boldsymbol{H}} = \boldsymbol{A}\tilde{\boldsymbol{H}}. \end{aligned} \quad (28)$$

The matrix inversion operation associated with the process of evaluating the estimator matrix $\boldsymbol{A}$ in Equation (28) cannot be avoided as opposed to the case of the SS-CIR estimation scheme of Section III-B. However, the estimator matrix $\boldsymbol{A}$ is data-independent and it is sufficient to calculate it once for the case of encountering Wide Sense Stationary (WSS) channel statistics.

The corresponding covariance matrix associated with the FS-CIR estimate vector $\hat{\boldsymbol{\alpha}}$ may be expressed as [6]

$$\boldsymbol{C}_\alpha = \sigma_v^2 \left(\sigma_v^2 \boldsymbol{I} + \mathrm{diag}\left(\sigma_l^2\right) \boldsymbol{T}^{\mathrm{H}} \boldsymbol{T}\right)^{-1} \mathrm{diag}\left(\sigma_l^2\right) \quad (29)$$

and the resultant Normalized Mean Square Error (NMSE) of the RC-MMSE FS-CIR estimator proposed is given by

$$NMSE_\alpha = \frac{\sigma_v^2}{\sigma_H^2} \mathrm{trace}\left(\left(\sigma_v^2 \boldsymbol{I} + \mathrm{diag}\left(\sigma_l^2\right) \boldsymbol{T}^{\mathrm{H}} \boldsymbol{T}\right)^{-1} \mathrm{diag}\left(\sigma_l^2\right)\right), \quad (30)$$

where $tr(\boldsymbol{A})$ is the *trace* of the matrix $\boldsymbol{A}$.

In order to complete the DDCE scheme of Figure 2 we employ the *a priori* CIR predictor as derived in [1]. The CIR predictor considered can be implemented in conjunction with both the SS-CIR and the FS-CIR estimators of Sections III-B and III-C, respectively. However, in the case of encountering a fractionally-spaced CIR, the effective SS-CIR taps $h[n,m]$ of Equation (6) can no longer be assumed uncorrelated for different values of the index m, as advocated in Section II-A. Thus the performance of the *a priori* CIR predictor described here in conjunction with the SS-CIR estimator will deviate from that reported in [1].

IV. Simulation Results

In this section, we present our simulation results for both the Sample-Spaced and the Fractionally-Spaced RC-MMSE CIR estimation schemes advocated in the context of both OFDM and MC-CDMA systems communicating over eight-path dispersive Rayleigh fading channel characterized in [7].

TABLE I
System parameters.

Parameter	OFDM	MC-CDMA
Channel bandwidth	800 kHz	
Number of carriers K	128	
Symbol duration T	160 μs	
Max. delay spread τ_{max}	40 μs	
No. of CIR taps	3	
Channel interleaver	WCDMA [8] 248 bit	–
Modulation	QPSK	
Spreading scheme	–	WH
FEC component codes code interleaver	Turbo code [9] , rate 1/2 RSC, K=3(7,5) WCDMA (124 bit)	

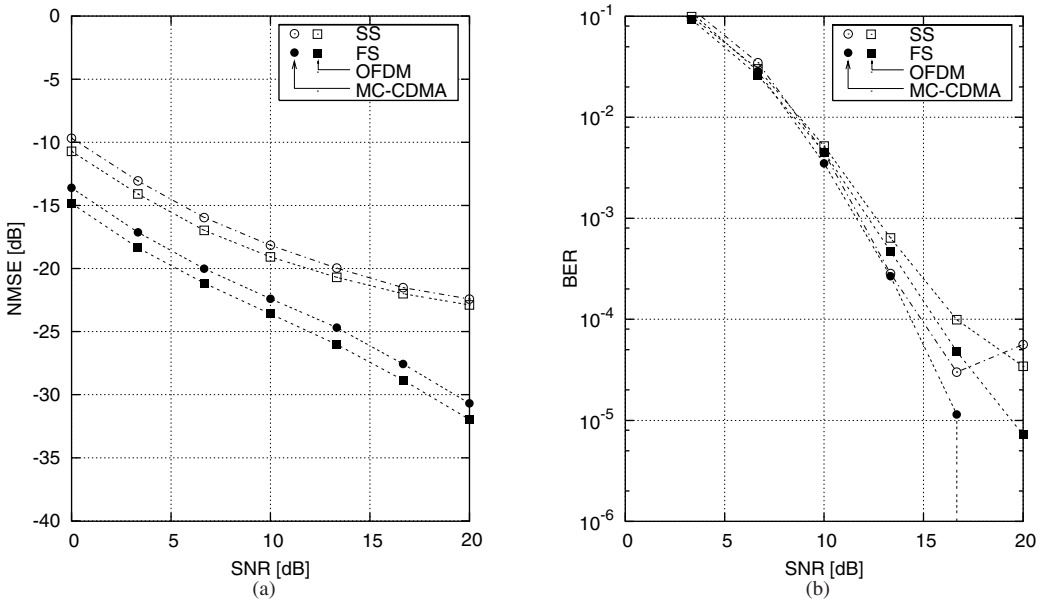

Fig. 3. (a) **NMSE** exhibited by the decision-directed channel estimator of Section III-A in the context of OFDM and MC-CDMA systems and (b) the corresponding achievable **BER** performance. Both performance curves are shown as a function of the average SNR at the reception antenna. The *frame-varient* fading channel characterized by Bug's channel model [7] were encountered at OFDM symbol-normilized Doppler frequency of $F_d = 0.01$.

Our simulations were performed in the base-band frequency domain and the system configuration characterised in Table I is to a large extent similar to that used in [4]. We assume having a total bandwidth of 800kHz. In the OFDM mode, the system utilises 128 QPSK-modulated orthogonal subcarriers. In the MC-CDMA mode we employ eight full sets of 16-chip Walsh-Hadamard (WH) codes for interleaved frequency-domain spreading of the QPSK-modulated bits over the 128 orthogonal subcarriers. All the 128 WH spreading codes, constituted by 8 interleaved groups of 16 codes each, are assigned to a single user and hence the data-rate is similar in both the OFDM and the MC-CDMA modes. For forward error correction (FEC) we use $\frac{1}{2}$-rate turbo coding [9] employing two constraint-length $K = 3$ Recursive Systematic Convolutional (RSC) component codes and a 124-bit WCDMA code interleaver [8]. The octally represented generator polynomials of (7,5) were used.

We employed the eight-path Rayleigh-fading Bug channel model characterised in [7], using the delay spread of $\tau_{rms} = 1\mu$s and the OFDM-symbol-normalized Doppler frequency of $F_D = 0.01$.

Figure 3(a) demonstrates the NMSE exhibited by the DDCE scheme of Figure 2 employing both the SS-CIR estimator described in Section III-B and the FS-CIR estimator derived in Section III-C in the context of both the OFDM and the MC-CDMA systems considered. The corresponding achievable Bit Error Rate (BER) performance is depicted in Figure 3(b). The simulations were carried out over the period of 100,000 QPSK-modulated $K = 128$-subcarrier OFDM/MC-CDMA symbols. It can be seen in Figure 3(a), that the DDCE employing the *a posteriori* FS-CIR RC-MMSE method outperforms its SS-CIR estimator-based counterpart over the entire range of the SNR values considered. Furthermore, the DDCE scheme utilizing the SS-CIR estimator exhibits an irreducible noise-floor at high SNR values. This effect can be explained by the fact that the *a priori* CIR predictor described in [1] fails to exploit the correlation between different SS-CIR taps. Furthermore, the statistics of the correlated SS-CIR taps diverges from the time-domain correlation model assumed by the predictor and described in Section II-A, which results in a biased estimation process.

V. Conclusions

In this paper we have analysed and compared the attainable performance of two DDCE schemes, namely the DDCE employing an *a posteriori* SS-CIR estimator derived in [2] and its FS-CIR estimator-based counterpart introduced here. The performance of both methods was explored in conjunction with realistic channel conditions characterized by a time-variant Rayleigh fading FS-CIR. We have shown that the latter estimation method exhibits substantial advantages in terms of both the achievable system performance and its robustness against the variations of the channel characteristics, such as the RMS delay spread. Additionally, we have demonstrated that the MC-CDMA system employing the proposed channel estimation scheme outperforms its OFDM counterpart.

References

[1] L. Hanzo, Münster, B. Choi, and T. Keller, *OFDM and MC-CDMA for Broadband Multi-user Communications, WLANs and Broadcasting*. John Wiley – IEEE Press, 2003, 992 pages.

[2] J. Akhtman and L. Hanzo, "Generic reduced-complexity MMSE channel estimation for OFDM and MC-CDMA," in *Proceedings of the Spring'05 IEEE Vehicular Technology Conference*, Stockholm, Sweden, May 2005.

[3] R. Steele and L. Hanzo, Eds., *Mobile Radio Communications*, 2nd ed. New York, USA: IEEE Press - John Wiley & Sons, 1999, 1090 pages.

[4] Y. Li, L. Cimini, and N. Sollenberger, "Robust channel estimation for OFDM systems with rapid dispersive fading channels," *IEEE Transactions on Communications*, vol. 46, no. 7, pp. 902–915, April 1998.

[5] Y. Li, "Pilot-Symbol-Aided Channel Estimation for OFDM in Wireless Systems," *IEEE Transactions on Vehicular Technology*, vol. 49, no. 4, pp. 1207–1215, July 2000.

[6] S. Kay, *Fundamentals of Statistical Signal Processing*. Englewood Cliffs, NJ, USA: Prentice-Hall, 1998.

[7] S. Bug, C. Wengerter, I. Gaspard, and R. Jakoby, "Channel model based in comprehensive measurements for DVB-T mobile applications," in *IEEE Instrumentation and Measurements Technology Conference*, Budapest, Hungary, May 21-23 2001.

[8] H. Holma and A. Toskala, Eds., *WCDMA for UMTS : Radio Access for Third Generation Mobile Communications*. John Wiley and Sons, Ltd., 2000.

[9] L. Hanzo, T. Liew, and B. Yeap, *Turbo Coding, Turbo Equalisation and Space-Time Coding*. Chichester, UK; Piscataway, NJ, USA: John Wiley, IEEE Press, 2002, 766 pages. (For detailed contents, please refer to http://www-mobile.ecs.soton.ac.uk.).